Self-assembly of acacia and β-lactoglobulin in aqueous dispersions

C. Schmidt, G. Mekloufi, Denis Renard, J. Hardy, Paul Robert, Christian Sanchez

HAL Id: hal-02832475

https://hal.inrae.fr/hal-02832475

Submitted on 7 Jun 2020

20. X. Qi, B. X. Behrens, P. R. West and A. E. Mort, *Plant Physiol.*, 1995, **108**, 1691.
21. J. D. Brady, I. H. Sadler and S. C. Fry, *Biochem. J.*, 1996, **315**, 323.
22. J. Sommer-Knudsen, A. Bacic and A. E. Clarke, *Phytochemistry*, 1998, **47**, 483.
23. M. J. Kieliszewski and D. T. A. Lamport, *Plant J.*, 1994, **5**, 157.
24. J. Chen and J. E. Varner, *EMBO J.*, 1985, **4**, 2145.
25. A. V. Dobrynin, R. H. Colby and M. Rubinstein, *Macromolecules*, 1995, **28**, 1859.
26. R. Skouri, F. Schosseler, J. P. Munch and S. J. Candau, *Macromolecules*, 1995, **28**, 197.
27. M. Rubinstein, R. H. Colby, A. V. Dobrynin and J.-F. Joanny, *Macromolecules*, 1996, **29**, 398.
28. P. J. Flory, *Principles of Polymer Chemistry*, Cornell University Press, 1953.
29. J.-L. Barrat and J.-F. Joanny, *Adv. Chem. Phys.*, 1996, **94**, 1.
30. G. S. Manning, *Berenges Phys. Chem.*, 1996, **100**, 923.
31. G. S. Manning and J. Ray, *J. Biomol. Struct. Dynamics*, 1998, **16**, 461.
32. V. A. Parsegian, R. P. Rand, N. L. Fuller and D. C. Rau, *Methods Enzymol.*, 1986, **127**, 400.
33. P. Ryden, A. J. MacDougall, C. W. Tibbits and S. G. Ring, *Biopolymers*, 2000, **54**, 398.
34. A. J. MacDougall, N. M. Rigby, P. Ryden, C. W. Tibbits and S. G. Ring, *Biomacromolecules*, 2001, **2**, 450.
35. A. D. Tomos and R. A. Leigh, *Ann. Rev. Plant Physiol. Plant Mol. Biol.*, 1999, **50**, 447.
36. K. A. Shackel, C. Greve, J. M. Labavitch and H. Ahmadi, *Plant Physiol.*, 1991, **97**, 814.

Self-assembly of Acacia Gum and β-Lactoglobulin in Aqueous Dispersion

C. Sanchez,[1] C. Schmitt,[1,2] G. Mekhloufi,[1] J. Hardy,[1] D. Renard[3] and P. Robert[3]

[1]LABORATOIRE DE PHYSICO-CHIMIE ET GÉNIE ALIMENTAIRES, ENSAIA-INPL, BP172, 54505 VANDOEUVRE-LÈS-NANCY CEDEX, FRANCE
[2]PRESENT ADRESS: NESTLÉ RESEARCH CENTER, DEPARTMENT OF FOOD SCIENCE AND PROCESS RESEARCH, VERS-CHEZ-LES-BLANC, CH–1000 LAUSANNE 26, SWITZERLAND
[3]UNITÉ DE PHYSICO-CHIMIE DES MACROMOLÉCULES, INRA, BP 71627, 44316 NANTES CEDEX 3, FRANCE

1 Introduction

Complex coacervation is a liquid–liquid or, in some cases, liquid–solid phase separation which may be described basically by the formation of primary soluble macromolecular complexes that interact to form electrically neutralised aggregates, then unstable liquid droplets and/or precipitates that ultimately sediment to form the coacervated phase containing both biopolymers.[1–5] From a practical point of view, complex coacervation may be used in microencapsulation processes, in the formation of extracellular matrices for biomaterials design, in biotechnology (treatment of food processing waste and activated sludge, protein purification, biosensor design) and in the creation of new multifunctional food ingredients. A better knowledge of complex coacervation could also provide fundamental informations on important biological self-assembly processes such as DNA–protein interactions, cell cytosol organisation or tissue formation.

A survey of the abundant literature shows clearly that pH, ionic strength, type of ions, protein to polysaccharide ratio, size, shape, charge density and flexibility of macromolecules are important parameters controlling the extent of phase separation as determined at equilibrium.[3,4,6–10] On the contrary, out of equilibrium conditions have attracted much less attention. Some important questions such as the transition from macromolecular complexes/aggregates to the appearance of coacervates, the structure of coacervates and the phase ordering kinetics

from their appearance to the equilibrium remain to be elucidated.

A preliminary kinetic approach showed that a complex interplay between growth, coalescence/flocculation and sedimentation of coacervates occurred in the β-lactoglobulin acacia gum system.[11,12] More detailed structural and kinetic informations on this model system are reported in the following using confocal scanning laser microscopy and time resolved small angle static laser light scattering.

2 Materials and Methods

2.1 Materials

Acacia gum sample from *Acacia senegal* trees (lot 97J716) was a gift from the CNI company (Rouen, France). Acid processed β-lactoglobulin (lot 818) was a gift from Lactalis Research Center (Retiers, France). The chemical composition of powders and physico-chemical properties of acacia gum (AG) and β-lacto-globulin (BLG) macromolecules were reported previously.[13–16]

2.2 Preparation of BLG/AG Mixed Dispersions

AG and BLG aqueous stock dispersions at 0.1 wt% or 1 wt% total biopolymer concentration were prepared in deionized water (MilliQ, MilliPore, USA) or bidistilled water, respectively.[12] The pH of the resulting dispersions was adjusted to 3.6 or 4.2 using HCl or NaOH. BLG/AG dispersions at protein to polysac-charide weight ratios (Pr:Ps) of 1:1 or 2:1 were obtained by gently mixing stock dispersions. For light scattering experiments, stock dispersions were filtered through 0.22 μm Millex microfilters (MilliPore, USA) before mixing.

2.3 Confocal Scanning Laser Microscopy (CSLM)

The structure of BLG/AG mixtures at 1 wt% total biopolymer concentration was determined by CSLM. The procedure for BLG and AG labelling, respective-ly by FITC and RITC, and the technical set-up were described previously.[12] The focal plane of observation was about 30 μm from the inverted objective from the microscope. Pictures were processed $\sim$ 160 s after mixing stock dispersions using the Laser Sharp MRC–1024 software version 3.2 (Bio-Rad, Germany). In order to better visualize microstructures, pictures were transformed in negative images and brightness and contrast were optimized using the imagoWeb free-ware version 1.1.[17] All experiments were duplicated using freshly prepared dispersions.

2.4 Small Angle Static Laser Light Scattering (SALS)

Phase ordering kinetics of BLG/AG mixtures at 0.1 wt% total biopolymer concentration, 2:1 Pr:Ps weight ratio and pH 4.2 were followed during 90 min using SALS. Light scattering experiments were carried out using a Mastersizer S

long bench (Malvern Ltd, UK). A He–Ne laser light ($\lambda = 0.6334\,\mu$m) was passed through a 0.5 mm width measurement cell (Malvern Ltd) in which the BLG/AG mixture was injected using a syringe. The beam was converged by a Reverse Fourier 300 mm focussing lens. 42 Detectors, covering a scattering wave vector Q range of 8×10^{-3} to 10 μm^{-1}, collected the scattered light. Experimental scattering intensity was obtained every 30 s (sample time: 10 s) by substracting the background intensity (cell + filtered MilliQ water) from the raw scattered intensity of the sample. In addition, corrections were applied to take into account the geometry of the detectors. The resulting scattered intensity was further corrected for turbidity.[18] Experiments were duplicated using freshly prepared dispersions.

3 Results and Discussion

3.1 Confocal Scanning Laser Microscopy (CSLM)

The microstructure of BLG/AG dispersions at 1:1 or 2:1 Pr:Ps weight ratios, pH 3.6 or 4.2 is shown Figure 1. A first look at the micrographs clearly shows that both pH and Pr:Ps weight ratio have a pronounced influence on the initial microstructure of mixed dispersions. At 1:1 Pr:Ps, a great number of polydisper-sed coacervates appeared. The apparent diameters (d_{app}) of coacervates ranged
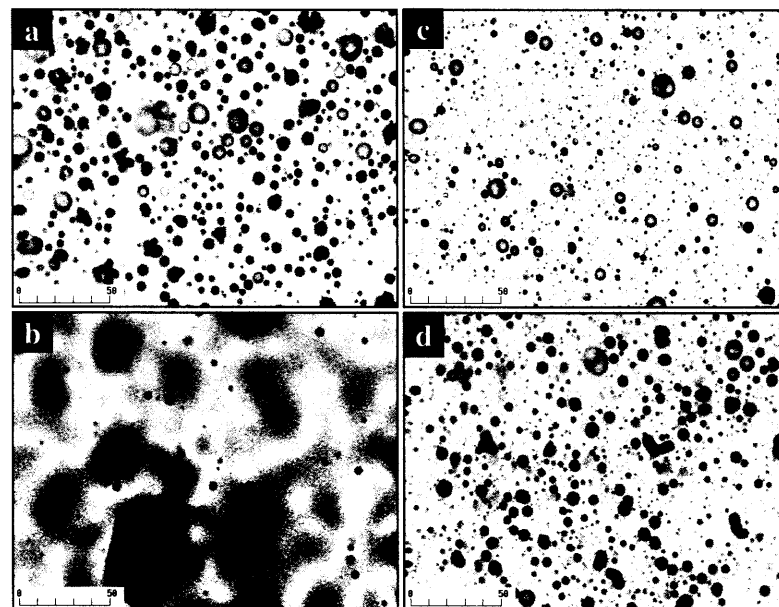

Figure 1 *CSLM micrographs obtained on BLG/AG dispersions at 1 wt% total biopolymer concentration, pH 3.6 (a, b) or 4.2 (c, d) and Pr:Ps weight ratios of 1:1 (a, c), 2:1 (b,d). Scale bar refers to 50 μm*

from 1 to 30 μm at pH 3.6 and from 1 to 20 μm at pH 4.2 (Figure 1a, c). Most coacervates displayed a d_{app} in the range 5–10 μm and 1–5 μm at pH 3.6 and 4.2, respectively. This is a clear indication that BLG/AG dispersions at pH 3.6 were less stable than at pH 4.2. A likely reason is that coacervates in the former case were electrically neutral, which favours flocculation/coalescence phenomena, whereas they were negatively charged in the latter case, which favours particle stabilization through charge repulsion.[14] An interesting feature was the presence of vesicular or multivesicular coacervates for both pH (Figure 1a, c). Similar structures have been observed in a preliminary CSLM study.[12] The origin of such structures remains unclear. However, very similar giant vesicles induced by self-assembly of polymers have been shown by CSLM.[19] One hypothesis would be the micellization of a macrosurfactant formed by interactions between AG and BLG. It is possible that the high molecular mass surface-active Arabinogalactan-Protein (AGP) component of AG plays a key role in the appareance of vesicles. We plan in the future to verify the latter hypothesis by separating the different molecular fractions of AG.

At 2:1 Pr:Ps ratio, BLG/AG dispersions at pH 3.6 were less stable than at pH 4.2 (Figure 1b, d). A rapid sedimentation of insoluble coacervates onto the observation slide was the result of this instability (dark areas in Figure 1b). At pH 4.2, vesicular coacervates were present and a number of flocculation/coalescence phenomena between coacervates were visible. As a general trend, BLG/AG dispersions at 2:1 Pr:Ps ratio were less stable than at ratio 1:1. For instance, size distribution of coacervates was in the range 1–5 μm at ratio 1:1 and rather in the range 5–10 μm at ratio 2:1. This may be explained by the better charge neutralization of coacervates in the latter case.[14]

3.2 Small Angle Static Light Scattering (SALS)

When a binary mixture is quenched in the unstable coexistence region, by thermal treatment or pressure changes or simply by mixing the two macromolecules, fluctuations in density grow with time, and finally result in a complete phase separation. The dynamics of phase separation are generally divided into early, intermediate and late stages. The different stages can be described by means of the temporal evolution of the scattered intensity function.[20–22]

The scattered intensity function initially displayed a correlation peak at a correlation length Λ ($\Lambda = 2\pi/Q_{max}$ where Q_{max} is the scattering wave vector corresponding to the maximum scattered intensity I_{max}) of 19 μm (Figures 2, 3). In the time interval between 0 and 1350 s, Q_{max} shifted towards smaller Q values indicating the growth of structural domains. The presence of a correlation peak is generally ascribed to the spinodal decomposition phase separation mechanism.[20,21] This feature can be observed for the nucleation and growth mechanism when numerous particles or when depleted areas around growing particles are present.[22,23] The evolution of the correlation length Λ is shown in Figure 3. Following a short lag time, Λ increased from 15–19 μm (t = 0 s) up to 45 μm (t = ~ 700–800 s). After ~ 700–800 s, the correlation length reached a constant value but the system coarsening continued, in agreement with the increase of
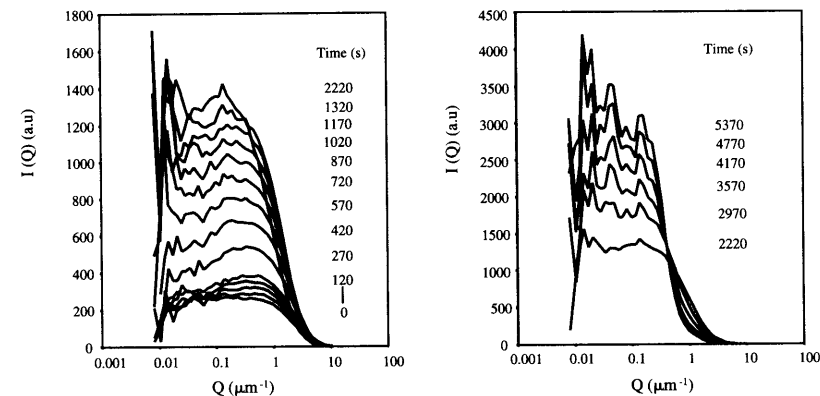
Figure 2 *Temporal evolution of scattered intensity functions [I(Q) vs Q] as determined by SALS on BLG/AG dispersions at 0.1 wt% total biopolymer concentration, pH 4.2 and Pr:Ps weight ratio of 2:1*
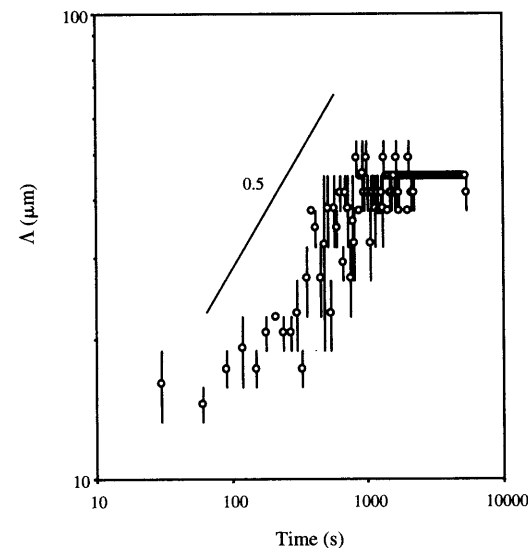

Figure 3 *Temporal evolution of the correlation length Λ (μm) as determined by SALS on BLG/AG dispersions at 0.1 wt% total biopolymer concentration, pH 4.2 and Pr:Ps weight ratio of 2:1. Bars are standard deviation based on duplicate experiments. Drawn line is a power-law function with an exponent of 0.5*

scattered intensity at small Q (Figure 2). The increase of Λ as a function of time followed a power-law relationship $Q_{max} \sim t^{-\alpha}$ with α equal to ~ 0.4–0.5 (Figure 3). This value is intermediate between that obtained for diffusion-induced coalescence ($\alpha = 0.33$) and that obtained for hydrodynamics-induced coarsening ($\alpha = $
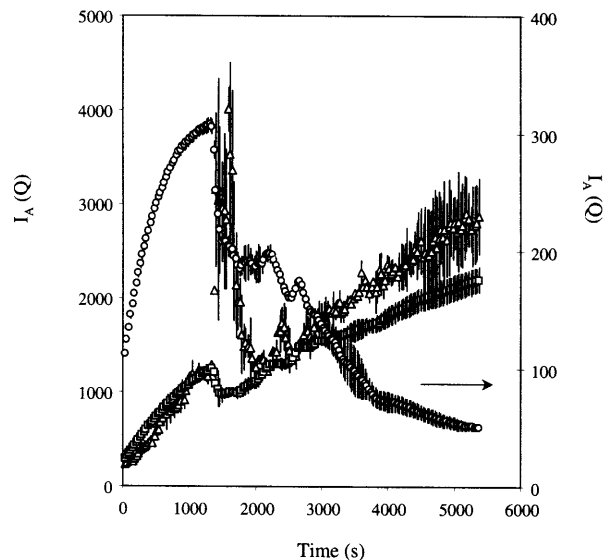
Figure 4 *Temporal evolution of scattered intensities $I_A(Q)$ averaged according to three Q ranges to distinguish large, medium and small sized particles as determined by SALS on BLG/AG dispersions at 0.1 wt% total biopolymer concentration, pH 4.2 and Pr:Ps weight ration of 2:1. [△]: large particles (Q: 0.008–0.042 μm^{-1}), [□]: medium particles (Q: 0.05–0.67 μm^{-1}), [○]: small particles (Q: 0.8–10.4 μm^{-1}). Bars are standard deviation based on duplicate experiments*

1), indicating a correlation between growth mechanisms.[24]

Coarsening kinetics can be better visualized by averaging the scattered intensities according to three ranges of Q. The three ranges were assigned to large, medium and small sized particles (Figure 4). Following a first phase (0–1320 s) where an increasing number of polydispersed droplets appeared, a sudden increase of large particles was observed in parallel with a decrease of medium and small particles (1350–1380 s). This large-scale coalescence/flocculation process could be at the origin of the formation of multivesicular structures. In a second step, large particles disappeared due to gravity effects (sedimentation) or adsorption onto glass walls of optical cell or collapse of structures. A transition regime appeared between ∼ 1800 and ∼ 2300 s where the number of large particles still decreased but the number of medium and small particles increased again. The observation was important since it suggests that different coarsening rates exist in the system, probably stemming from the different molecular masses or charge densities of AG molecular fractions. It is known, for instance, that large polymers induced faster phase separation than smaller ones.[3] Finally, small particles decreased to a large extent to the benefit of medium and large particles that grew continuously.

As the shape of the different scattered intensity functions and the power-law growth of structural domains suggested that the system was located in the late

stage regime of the phase separation, SALS data were scaled by plotting I/I_{max} *vs* Q/Q_{max}.[23] Unfortunately, scaled data did not overlap into a single master curve (results not shown). Possible explanations would be that more than one length scale occurred in the phase separating system (effect of polydispersity) or that the final stage characterized by sharp interfaces was not reached. According to the Porod law, scattering arising from sharp interfaces should produce a high-Q tail decreasing as Q^{-4}.[24] In our system, the scaling law exponent varied with time from 2.9 to 3.6, indicating that coarsening of droplets with time is coupled with a reorganisation of droplets interfaces.

4 Conclusion

Complex coacervation between BLG and AG induced the formation of supra-molecular structures such as droplets, vesicles or multihollow spheres. SALS experiments demonstrated the presence of a decomposition process with correlated growth mechanisms. Coarsening kinetics were mainly characterized by an interplay between initial particles growth, large-scale flocculation/coalescence and transient growth of small particles. Polydispersity of particles size and roughness of interfaces precluded from applying dynamic scaling of the structure function.

Acknowledgements

References

1. H. G. Bungenberg de Jong, *Colloid Science*, H. R. Kruyt (ed.), Elsevier, Amsterdam, 1949, Vol. 2, p. 233.
2. V. B. Tolstoguzov, *Food Proteins and their Applications*, S. Damodaran and A. Paraf (eds.), Marcel Dekker, New York, 1997, Chapter 6, p. 171.
3. C. Schmitt, C. Sanchez, S. Desobry-Banon and J. Hardy, *Crit. Rev. Food Sci. Nutr.*, 1998, **38**, 689.
4. K. W. Mattison, Y. Wang, K. Grymonpré and P. L. Dubin, *Macromol. Symp.*, 1999, **140**, 53.
5. K. Kaibara, T. Okazaki, H. B. Bohidar and P. L. Dubin, *Biomacromolecules*, 2000, **1**, 100.
6. V. B. Tolstoguzov, *Food Hydrocoll.*, 1991, **4**, 429.
7. D. J. Burgess, *Macromolecular Complexes in Chemistry and Biology*, P. L. Dubin, J. Bock, R. Davis, D. N. Schulz and C. Thies (eds.), Springer Verlag, Berlin, 1994, Chapter 17, p. 281.
8. J. Xia and P. L. Dubin, *Macromolecular Complexes in Chemistry and Biology*, P. L. Dubin, J. Bock, R. Davis, D. N. Schulz and C. Thies (eds.), Springer Verlag, Berlin, 1994, Chapter 15, p. 247.
9. L. Piculell, K. Bergfeldt and S. Nilsson, *Biopolymer Mixtures*, S. E. Harding, S. E. Hill

and J. R. Mitchell (eds.), Nottingham University Press, Nottingham, 1995, Chapter 2, p. 13.

10. J.-L. Doublier, C. Garnier, D. Renard and C. Sanchez, *Curr. Opin. Colloid Interf. Sci.*, 2000, **5**, 184.

11. C. Sanchez, S. Despond, C. Schmitt and J. Hardy, *Food Colloids: Fundamentals of Formulation*, E. Dickinson and R. Miller (eds.), Royal Society of Chemistry, Cambridge, 2001, p. 332.

12. C. Schmitt, C. Sanchez, A. Lamprecht, D. Renard, C. M. Lehr, C. G. de Kruif and J. Hardy, *Coll. Surf. B: Biointerf.*, 2001, **20**, 267.

13. C. Schmitt, PhD Thesis, INPL, Vandœuvre-lès-Nancy, France, 2000.

14. C. Schmitt, C. Sanchez, F. Thomas and J. Hardy, *Food Hydrocoll.*, 1999, **13**, 483.

15. C. Schmitt, C. Sanchez, S. Despond, D. Renard, F. Thomas and J. Hardy, *Food Hydrocoll.*, 2000, **14**, 403.

16. C. Sanchez, D. Renard, P. Robert, C. Schmitt and J. Lefebvre, *Food Hydrocoll.*, 2001, (submitted).

17. http://fabrizio.jth.it

18. T. Hashimoto, M. Itakura and H. Hasegawa, *J. Chem. Phys.*, 1986, **85**, 6118.

19. F. Ilhan, T. H. Galow, M. Gray, G. Clavier and V. M. Rotello, *J. Am. Chem. Soc.*, 2000, **122**, 5895.

20. F. Mallamace and N. Micali, *Light Scattering – Principles and Development*, W. Brown (ed.), Clarendon Press, Oxford, 1996, Chapter 12, p. 381.

21. J. K. G. Dhont, *J. Chem. Phys.*, 1996, **105**, 5112.

22. K. Binder, *Materials Science and Technology – A Comprehensive Treatment*, R. W. Cahn, P. Haasen and E. J. Kramer (eds.), VCH, Weinhem, 1991, Vol. 5, Chapter 7, p. 405.

23. J. Maugey, T. van Nuland and P. Navard, *Polymer*, 2001, **42**, 4353.

24. H. Furukawa, *Adv. Phys.*, 1985, **34**, 703.

Creation of Biopolymeric Colloidal Carriers Dedicated to Controlled Release Applications

Denis Renard,[1] Paul Robert,[1] Laurence Lavenant,[1] Dominique Melcion,[1] Yves Popineau,[1] Jacques Guéguen,[1] Cécile Duclairoir,[2] Evelyne Nakache,[2] Christian Sanchez[3] and Christophe Schmitt[4]

[1]INRA CENTRE DE RECHERCHES DE NANTES, RUE DE LA GERAUDIERE, BP 71627 44316 NANTES CEDEX 3, FRANCE
[2]EQUIPE POLYMERES INTERFACES LCMT, UMR 6507 ISMRA, 14050 CAEN CEDEX, FRANCE
[3]LPCGA ENSAIA/INPL, 54505 VANDOEUVRE-LES-NANCY, FRANCE
[4]NESTLE RESEARCH CENTER, CH–1000 LAUSANNE 26, SWITZERLAND

1 Introduction

In the last decade, micro and nanosized colloidal carriers have received a growing scientific and industrial interest.[1] These vectors may be capsules (with liquid core surrounded by a solid shell), particles (polymeric matrices), vesicles or liposomes, or multiple or single emulsions, and have found a wide range of applications. They may be loaded by living cells, enzymes, flavour oils, pharmaceuticals, vitamins, adhesives, agrochemicals or catalysts and offer considerable advantages in use. Liquids can be handled as solids, odour or taste can be effectively masked in a food product, sensitive substances can be protected from deleterious effects of the surrounding environment, toxic materials can be safely handled, and drug delivery can be controlled and targeted.[2]

In the forementioned laboratories, we started with a new strategy based on phase separation in order to prepare natural particles. Simple or complex coacervation methods involving proteins or protein and polysaccharide mixtures[3] were used to create new matrices dedicated to controlled release applications. The colloidal carriers produced were in the micrometre or nanometre size range depending on the substrates or the methods used. Wheat proteins, gliadins, were implicated in simple coacervation to produce nanospheres. Controlled release experiments with model compounds were conducted in order to evaluate